Second Virial Coefficient and Gyration-Radius Expansion Factor of Oligo- and Polystyrenes near the Θ Temperature. Solvent Dependence

Munenori Yamada, Takenao Yoshizaki, and Hiromi Yamakawa*

Department of Polymer Chemistry, Kyoto University, Kyoto 606-8501, Japan

Received May 26, 1998

ABSTRACT: The second virial coefficient A_2 was determined for atactic oligo- and polystyrenes in methyl acetate below, at, and above Θ (41.5 °C) in the range of weight-average molecular weight M_w from 4.74 × 10^2 (tetramer) to 7.72 × 10^6. The gyration-radius expansion factor α_S was also determined for the sample with $M_w = 7.72 \times 10^6$. It is found that A_2 depends on M_w appreciably in the range of small M_w. Although the dependence of A_2 on M_w in methyl acetate is different from that previously found in cyclohexane, the former may also be explained quantitatively by the Yamakawa theory that takes account of the effect of chain ends, indicating that the difference in the M_w dependence between A_2 in the two Θ solvents arises from that between the effects of chain ends. An analysis gives values of the effective excess binary-cluster integrals β_1 and β_2 associated with the chain end beads and also the binary-cluster integral β between intermediate identical beads as functions of temperature T, all of them except for β above Θ being quadratic in $\tau = 1 - \Theta/T$. With these values of β, the conventional and scaled excluded-volume parameters z and $\tilde{z}$ below Θ are calculated. The results for the part $A_2^{(HW)}$ of A_2 without the effect of chain ends along with those previously determined in cyclohexane give a single-composite curve below Θ when $A_2^{(HW)} M_w^{1/2}$ is plotted against z, being consistent with the two-parameter theory prediction irrespective of the difference in solvent condition. This is in contrast to the behavior of $A_2^{(HW)}$ above Θ. It is also found that if α_S is plotted against $\tilde{z}$ (or z for large M_w), the present data points along with those in cyclohexane form a single-composite curve, indicating that the quasi-two-parameter theory is valid for α_S below Θ as well as above Θ irrespective of the difference in solvent condition.

Introduction

In the previous experimental study[1] of the second virial coefficient A_2 of atactic oligo- and polystyrenes (a-PS) in cyclohexane near the Θ temperature (34.5 °C) within the framework of polymer solution theory recently developed on the basis of the helical wormlike (HW) chain,[2] it was found that the binary-cluster integral β (between intermediate beads) is not proportional to $1 - \Theta/T \equiv \tau$ with T the absolute temperature but quadratic in τ below Θ in contrast to the result above Θ that $\beta \propto \tau$. This unexpected finding has overturned the prevailing view that β is proportional to τ both above and below Θ for all polymer−solvent systems. Note that this is, of course, the case with some systems, for instance, atactic poly(methyl methacrylate) (a-PMMA) in acetonitrile.[3] It was then shown that the inconsistency of the experimental results for A_2 below Θ with the two-parameter (TP) theory prediction[4] previously[5,6] claimed may be regarded as arising from both the effect of chain ends and the incorrect assumption of the proportionality of β to τ. This leads to the conclusion that the molecular-weight M independence of A_2 as observed for a-PS[5] below Θ for relatively large M is due to an accidental cancellation of the M dependence of $A_2^{(HW)}$ by that of $A_2^{(E)}$, where $A_2^{(E)}$ represents the contribution of the effect of chain ends to A_2 and $A_2^{(HW)}$ is the part of A_2 without this effect. As for the gyration-radius expansion factor α_S below Θ, it was found to follow the TP or quasi-two-parameter (QTP) theory if the (intramolecular) conventional and scaled excluded-volume parameters[2,4] z and $\tilde{z}$ are calculated with the values of β determined as above.[1] (Recall that the QTP theory is valid for α_S above Θ.[2])

In order to examine whether the above findings for a-PS in cyclohexane are also the case with other Θ solvents, in the present work we make a similar study of this polymer in another Θ solvent, methyl acetate. Thus the purposes of the present paper are 2-fold. The first is to determine the dependence of β on τ near the Θ temperature directly from experimental data for A_2 for oligomer samples following the procedure previously established.[1] The second is to examine whether the present results for A_2 and α_S as functions of z and $\tilde{z}$ calculated with the values of β thus determined are consistent with the previous ones in cyclohexane.

Experimental Section

Materials. All the a-PS samples used in this work are the same as those used in the previous studies of the mean-square optical anisotropy $\langle\Gamma^2\rangle$,[7] the intrinsic viscosities $[\eta]_\Theta$[8] and $[\eta]$,[9,10] the mean-square radii of gyration $\langle S^2\rangle_0$[11] and $\langle S^2\rangle$,[12] the scattering function P_s,[13] the translational diffusion coefficients D_Θ[14] and D,[15,16] A_2 (or Ψ),[1,17,18] and the first cumulant Ω,[19] i.e., the fractions separated by preparative gel permeation chromatography (GPC) or fractional precipitation from the standard samples supplied by Tosoh Co., Ltd. All the samples have a fixed stereochemical composition (the fraction of racemic diads $f_r = 0.59$) independent of molecular weight, possessing an n-butyl group at one end of the chain (the initiating end) and a hydrogen atom at the other (the terminating end).

The values of the weight-average molecular weight M_w, the weight-average degree of polymerization x_w, and the ratio of M_w to the number-average molecular weight M_n are listed in Table 1. As seen from the values of M_w/M_n, all the samples except F850-a are very narrow in molecular weight distribution, and in particular, the samples OS4 and OS5 are completely monodisperse. We note that the value of M_w/M_n for F850-a could not be determined with high accuracy because of the lack of the GPC calibration curve in the necessary range.

The solvent methyl acetate was purified following the procedure of Chu et al.,[20] i.e., by drying for 1 or 2 days with anhydrous magnesium sulfate and subsequent distiration with diphosphorus pentaoxide prior to use.

10.1021/ma980833y CCC: $15.00
Published on Web 10/16/1998

Table 1. Values of M_w, x_w, and M_w/M_n for Atactic Oligo- and Polystyrenes

sample	M_w	x_w	M_w/M_n
OS4[a]	4.74×10^2	4	1.00
OS5	5.78×10^2	5	1.00
OS6	6.80×10^2	5.98	1.00
OS8a[b]	9.20×10^2	8.29	1.01
A2500a-2	2.83×10^3	26.7	1.03
A5000-3[c]	5.38×10^3	51.2	1.03
F1a-2	9.98×10^3	95.4	1.03
F2-2	2.02×10^4	194	1.02
F4	4.00×10^4	384	1.02
F40	3.59×10^5	3450	1.01
F80a-2[d]	7.32×10^5	7040	1.03
F128a-2[d]	1.27×10^6	12200	1.03
F288a-2	3.47×10^6	33400	1.05
F850-a	8.04×10^6	77300	

[a] M_w's of OS4, OS5, and OS6 had been determined by GPC.[7] [b] M_w's of OS8a through F850-a except for A5000-3, F80a-2, and F128a-2 had been determined from LS in cyclohexane at 34.5 °C.[10,11,16,19] [c] M_w of A5000-3 had been determined from LS in methyl ethyl ketone at 25.0 °C.[7] [d] M_w's of F80a-2 and F128a-2 had been determined from LS in benzene at 25.0 °C.[10]

Light Scattering. Light scattering (LS) measurements were carried out to determine A_2 for all the a-PS samples and $\langle S^2 \rangle$ for some of them in methyl acetate at various temperatures ranging from 30.0 to 50.0 °C. A Fica 50 light-scattering photometer was used for all the measurements with vertically polarized incident light of wavelength 436 nm. For a calibration of the apparatus, the intensity of light scattered from pure benzene was measured at 25.0 °C at a scattering angle of 90°, where the Rayleigh ratio $R_{Uu}(90°)$ of pure benzene was taken as 46.5×10^{-6} cm^{-1}. The depolarization ratio ρ_u of pure benzene at 25.0 °C was determined to be 0.41 ± 0.01 by the method of Rubingh and Yu.[21]

The conventional method was used for solutions of the samples with $M_w > 10^3$, while the procedure previously[22] presented was applied to those of the oligomer samples with $M_w < 10^3$ as before[1,3,18,23] since then the concentration dependences of the density scattering R_d and the optical constant K have significant effects on the determination of A_2 (and also of M_w). In order to determine A_2 by the latter procedure, we measured the reduced total intensity R^*_{Uv} of the unpolarized scattered light for vertically polarized incident light, the depolarization ratio ρ_u, the ratio $\kappa_T/\kappa_{T,0}$ of the isothermal compressibility of a given solution to that of the solvent, and the refractive index increment $(\partial\tilde{n}/\partial c)_{T,p}$ at constant temperature T and pressure p for the oligomer solutions, and also the first two quantities for the solvent. The values of the refractive index $\tilde{n}$ at finite concentrations c, which were required to calculate K, were calculated with the values of $(\partial\tilde{n}/\partial c)_{T,p}$ for each oligomer sample, as described in the Results. Measurements of R^*_{Uv} were carried out at scattering angles θ ranging from 37.5 to 142.5°, and the mean of the values obtained at different θ was adopted as its value, since it must be independent of θ for oligomers. The values of ρ_u were obtained by the same method as that employed in the calibration of the apparatus.

All the LS data obtained were analyzed by using the Berry square-root plot[24] and also the Bawn plot.[25,26] The correction for the anisotropic scattering was then applied to solutions of the samples with $M_w < 5 \times 10^3$.

The most concentrated solution of each sample except F850-a was prepared by continuous stirring at ca. 50 °C for 1−4 days. For F850-a, it was allowed to stand in the dark at ca. 50 °C for 7 days, being stirred by shaking the vessel gently twice a day. These solutions were optically purified by filtration through a Teflon membrane of pore size 1.0, 0.45, or 0.10 μm. The solutions of lower concentrations were obtained by successive dilution. The polymer mass concentrations c were calculated from the weight fractions with the densities of the solutions. The densities of the solvent and solutions were measured with a pycnometer of the Lipkin−Davison type.

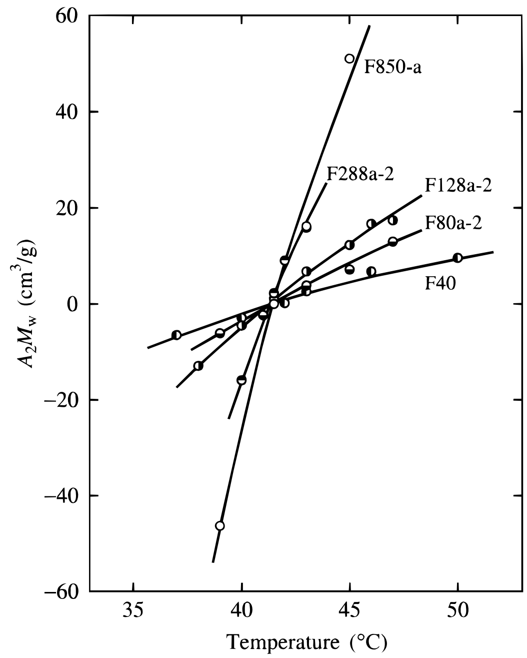

Figure 1. Plots of A_2M_w against temperature for the indicated a-PS samples in methyl acetate.

Isothermal Compressibility. Isothermal compressibility measurements were carried out to determine $\kappa_{T,0}$ of pure methyl acetate at 30.0, 41.5, and 50.0 °C. The apparatus and the method of measurements are the same as those described in the previous paper.[18] The ratio $\kappa_T/\kappa_{T,0}$ was determined as a function of c and p. The pressure p was varied from 1 to ca. 50 atm. In this range of p, it was independent of p within experimental error, so that we adopted the mean of the values obtained at various pressures as its value at 1 atm.

Refractive Index Increment. The refractive index increment $(\partial\tilde{n}/\partial c)_{T,p}$ at $c = 0$ was determined as a function of T for the samples OS4, OS5, OS6, OS8a, A2500a-2, and F2-2 at 30.0, 41.5, and 50.0 °C by the use of a Shimadzu differential refractometer.

Results

Θ Temperature. Figure 1 shows plots of A_2M_w against temperature for the five samples F40, F80a-2, F128a-2, F288a-2, and F850-a in methyl acetate, where the values of A_2 have been determined by using the Berry square-root plot.[24] Here we must make a remark on the sample F850-a, for which LS measurements were carried out at seven temperatures 33.0, 35.0, 37.0, 39.0, 41.5, 43.0, and 45.0 °C. The value of its M_w determined in this work is $(7.72 \pm 0.08) \times 10^6$ and ca. 4% smaller than the value 8.04×10^6 previously[19] determined in cyclohexane at 34.5 °C (see Table 1), indicating that the sample degraded somewhat in the course of preparation of its test solutions. Thus, in this paper we use the present value of its M_w for a data analysis.

It is seen from the figure that A_2 vanishes at almost the same temperature independent of M_w, leading to the conclusion that the Θ temperature is 41.5 °C for solutions of a-PS with $f_r = 0.59$ in methyl acetate. This value of Θ is somewhat lower than the corresponding value 43 °C determined by Chu et al.[20]

Light Scattering from Oligostyrene Solutions. We first give the values of $\kappa_T/\kappa_{T,0}$ and $(\partial\tilde{n}/\partial c)_{T,p}$ required to analyze the LS data for the samples with $M_w < 10^3$, as mentioned in the Experimental Section.

Considering the fact that $\kappa_T/\kappa_{T,0}$ for the oligomer samples at a given temperature is a linear function of

c, i.e.

$$\kappa_T/\kappa_{T,0} = 1 + kc \tag{1}$$

independently of M_w for both a-PS in cyclohexane[1] and a-PMMA in acetonitrile,[3] we may assume that this is also the case with a-PS in methyl acetate. On this assumption, the coefficient k in eq 1 at a given temperature may be calculated from the value of $\kappa_{T,0}$ for the pure solvent and that of κ_T for a-PS in the bulk. From the present experimental values $1.24_2 \times 10^{-3}$ and $1.49_1 \times 10^{-3}$ of $\kappa_{T,0}$ at 30.0 and 50.0 °C, respectively, and from the literature data obtained by Allen et al.[27] for a mixture of styrene oligomers including the dimer through the pentamer in the bulk and by Höcker et al.[28] for high-molecular-weight samples with $M_n = 5.1 \times 10^4$ and 8.2×10^4 in the bulk, k is calculated to be -0.603, -0.629, and -0.642 at 30.0, 41.5, and 50.0 °C, respectively. Here, the value of $\kappa_{T,0}$ at 41.5 °C and those of κ_T for a-PS in the bulk at 30.0, 41.5, and 50.0 °C have been estimated by interpolation. Thus we have determined the values of $\kappa_T/\kappa_{T,0}$ at temperatures ranging from 30.0 to 50.0 °C except at 41.5 °C by interpolation using eq 1 with the above values of k.

Next, considering the fact that $(\partial\tilde{n}/\partial c)_{T,p}$ may be expressed as a function of T by the equation

$$(\partial\tilde{n}/\partial c)_{T,p} = k_1 + k_2(T - \Theta) \tag{2}$$

independently of c in the relevant range of c for both a-PS in cyclohexane[1] and a-PMMA in acetonitrile,[3] we may assume that this is also the case with a-PS in methyl acetate. On this assumption, the coefficients k_1 and k_2 in eq 2 for a given sample may be calculated from the values of $(\partial\tilde{n}/\partial c)_{T,p}$ at $c = 0$ at a few temperatures. From the present experimental values of $(\partial\tilde{n}/\partial c)_{T,p}$ at $c = 0$ at 30.0, 41.5, and 50.0 °C, we have calculated k_1 and k_2 for the samples OS4,OS5, OS6, OS8a, A2500a-2, and F2-2 in methyl acetate at 436 nm. Then k_2 is independent of M_w but k_1 depends on M_w as in the previous cases of a-PS in cyclohexane[1] and a-PMMA in acetonitrile.[3] The values of k_1 are 0.222, 0.231_9, 0.234_6, 0.242_9, and 0.249_5 for OS4, OS5, OS6, OS8a, and A2500a-2, respectively. For the samples with $M_w \gtrsim 5 \times 10^3$, we use its value 0.248_0 obtained for F2-2. The value of k_2 is $(2.8 \pm 0.3) \times 10^{-4}$ cm^3/gK. The values of $\tilde{n}$ at finite c may be obtained from eq 2 by integration over c with the values of $\tilde{n}_0$ for pure methyl acetate at the respective temperatures corresponding to the LS measurements.

Now we may evaluate the excess Rayleigh ratio ΔR_0 for all the samples, including the oligomers, by the use of the values of $\kappa_T/\kappa_{T,0}$ and $(\partial\tilde{n}/\partial c)_{T,p}$ obtained above. Figure 2 shows as examples Berry square-root plots of ΔR_0 against c for the oligomer samples with $M_w \leq 9.98 \times 10^3$ in methyl acetate at 30.0 °C. The data points for each sample follow a curve concave upward, as shown by the solid curve (which represents the values calculated as described below). The results indicate that besides the second virial coefficient A'_2, the third virial coefficient A'_3 at least contributes appreciably to $Kc/\Delta R_0$ as c is increased. (Here, the prime attached to A_2 and A_3 indicates that they are the *light-scattering* virial coefficients.) It is then difficult to determine A'_2 from the plots with high accuracy.

Therefore, we have made Bawn plots. Figure 3 shows those plots for the four samples indicated as examples, where $S(c_i, c_j)$ is defined by eq 6 of ref 23. As seen from

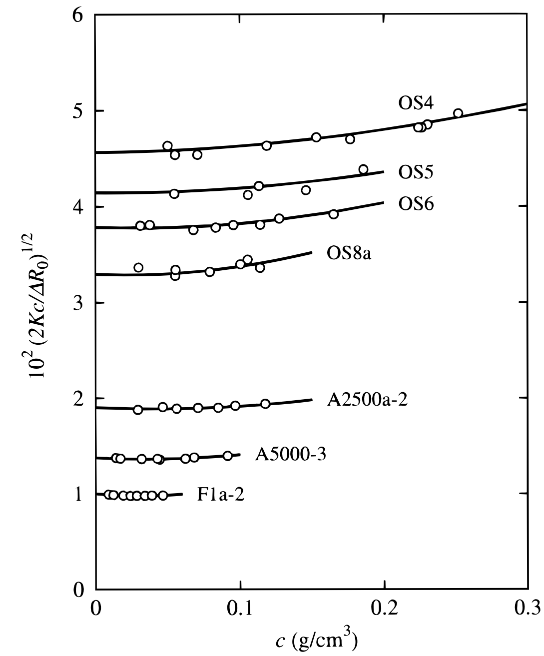

Figure 2. Plots of $(Kc/\Delta R_0)^{1/2}$ against c for the indicated a-PS samples in methyl acetate at 30.0 °C.

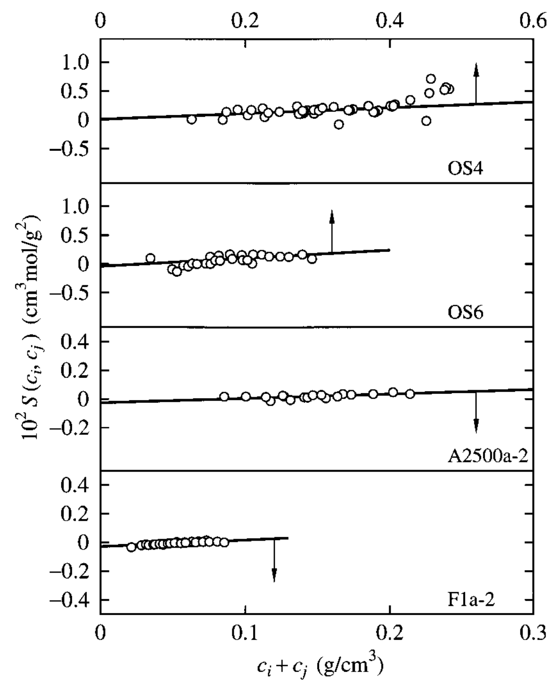

Figure 3. Bawn plots for the indicated a-PS samples in methyl acetate at 30.0 °C.

this figure, the data points for each sample follow a straight line, indicating that the terms higher than A'_3 may be neglected in the range of c studied. From the straight lines indicated, we have determined A'_2 and A'_3 for each sample in methyl acetate at 30.0 °C. Then, we have determined M_w of each sample so that the curve of $(Kc/\Delta R_0)^{1/2}$ calculated with these values of M_w, A'_2, and A'_3 may give a best fit to the data points in Figure 2. The solid curves in Figure 2 represent the values so calculated. The good fit of each curve to the corresponding data points indicates that M_w, A'_2, and A'_3 have been determined accurately.

Although the results are not shown here, the data at the other temperatures and for the samples F2-2 and

Table 2. Results for A_2 and $\alpha_S{}^2$ of Atactic Oligo- and Polystyrenes in Methyl Acetate

sample	30.0 °C	32.0 °C	33.0 °C	35.0 °C	37.0 °C	38.0 °C	39.0 °C	41.5 °C (Θ)	43.0 °C	45.0 °C	50.0 °C
						$10^4 A_2$, cm^3 mol/g^2					
OS4	0.5	1.3		2.0		2.5		3.3		4.3	5.3
OS5	−0.5	0.3		0.5		1.5		2.8		3.5	3.8
OS6	−2.0	−1.0		0.0		0.5		1.8		2.5	3.5
OS8a	−2.3	−1.8		−0.8		0.0		1.5		2.5	3.0
A2500a-2	−1.3	−1.1		−0.5		−0.1		0.1		0.7	0.8
A5000-3	-1.0_8	-0.8_0		-0.7_4		-0.3_3		-0.0_5		0.2_0	0.3_8
F1a-2	-1.4_5	-1.1_8		-0.7_3		-0.5_5		-0.1_8		0.0_3	0.0_7
F2-2	-0.7_6	-0.6_8		-0.5_6		-0.3_8		-0.0_4		0.1_0	0.1_4
F4	-0.5_6	-0.5_1		-0.3_9		-0.1_9		0.0_0		0.0_4	0.0_9
F850-a			-0.2_9	-0.2_2	-0.1_1		-0.0_6	0.0_0	0.0_2	0.0_7	
						$\alpha_S{}^2$					
F850-a			0.79_1	0.84_1	0.90_9		0.94_4	(1)	1.04_0	1.06_1	

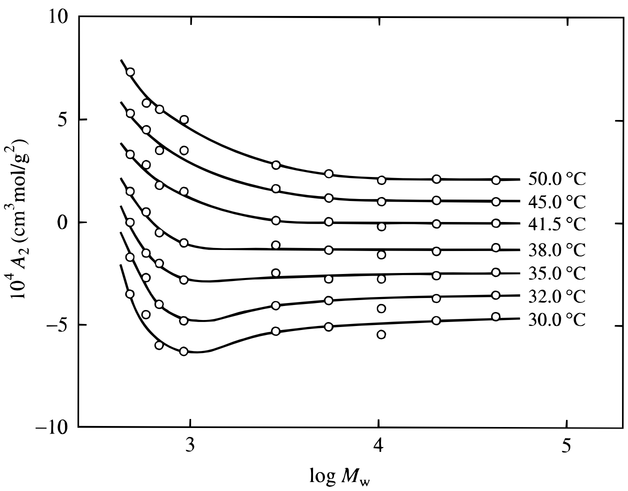

Figure 4. Plots of A_2 against log M_w for a-PS in methyl acetate at the temperatures indicated. The data points at 50.0 and 45.0 °C are shifted upward by 2 × 10^4 and 1 × 10^4 cm^3 mol/g^2, respectively, and those at 38.0, 35.0, 32.0, and 30.0 °C, downward by1 × 10^4, 2 × 10^4, 3 × 10^4, and 4 × 10^4 cm^3 mol/g^2, respectively. The solid curves connect the data points smoothly.

F4 have been analyzed by the same method, and the values of M_w, A'_2, and A'_3 have been determined with the accuracy comparable to the cases of Figures 2 and 3. It has then proved that the values of A'_2 so obtained may be equated to those of the (osmotic) second virial coefficient A_2 as in the case of the previous results at Θ.[18]

Second Virial Coefficient and Gyration-Radius Expansion Factor. In Table 2 are given the values of A_2 thus determined for the samples with $M_w \lesssim 4 \times 10^4$ in methyl acetate at temperatures ranging from 30.0 to 50.0 °C and also those of A_2 and α_S^2 determined for F850-a by using the Berry square-root plot.[24] Figure 4 shows plots of A_2 against log M_w for the samples with $M_w \lesssim 4 \times 10^4$ at the temperatures indicated, where the data points at 50.0 and 45.0 °C are shifted upward by 2 × 10^4 and 1 × 10^4 cm^3 mol/g^2, respectively, and those at 38.0, 35.0, 32.0, and 30.0 °C, downward by 1 × 10^4, 2 × 10^4, 3 × 10^4, and 4 × 10^4 cm^3 mol/g^2, respectively. The solid curves connect the data points smoothly.

In contrast to the previous case of a-PS in cyclohexane,[1] for which A_2 decreases monotonically with increasing M_w at all the temperatures investigated near Θ = 34.5 °C (see Figure 5 of ref 1), A_2 of a-PS in methyl acetate as a function of M_w has a distinct minimum at 32.0 and 30.0 °C. This difference may be regarded as arising from that between the effects of chain ends on A_2 in the two Θ solvents.

Discussion

Effects of Chain Ends on A_2. As done in the previous studies,[1,3] we analyze the data for A_2 in Table 2 by the use of the Yamakawa theory[2,6,29] that considers the effect of chain ends on the basis of the HW bead model. For convenience, we begin by summarizing the necessary basic equations. The model is such that $n + 1$ beads are arrayed with spacing a between them along the contour of total length $L = na$, where the $n - 1$ intermediate beads are identical and the two end ones are different from the intermediate ones and also from each other in species. Identical excluded-volume interactions between intermediate beads are expressed in terms of the conventional binary-cluster integral β, while two kinds of effective excess binary-cluster integrals β_1 and β_2 are necessary in order to express interactions between unlike beads, β_1 being associated with one end bead and β_2 with two end ones. The HW model itself[2] is defined in terms of the three basic model parameters: the constant differential-geometrical curvature κ_0 and torsion τ_0 of its characteristic helix taken at the minimum zero of its elastic energy and the static stiffness parameter λ^{-1}.

According to the theory,[2,6,29] A_2 in general may be written in the form

$$A_2 = A_2^{(\mathrm{HW})} + A_2^{(\mathrm{E})} \tag{3}$$

where $A_2^{(\mathrm{HW})}$ is that part of A_2 without the effect of chain ends which vanishes at Θ, and $A_2^{(\mathrm{E})}$ represents the contribution of this effect to A_2. The first term $A_2^{(\mathrm{HW})}$may be written as

$$A_2^{(\mathrm{HW})} = (N_A c_\infty{}^{3/2} L^2 B / 2M^2) h \tag{4}$$

where N_A is the Avogadro constant, and c_∞ and B are given by

$$c_\infty = \frac{4 + (\lambda^{-1}\tau_0)^2}{4 + (\lambda^{-1}\kappa_0)^2 + (\lambda^{-1}\tau_0)^2} \tag{5}$$

and

$$B = \beta / a^2 c_\infty{}^{3/2} \tag{6}$$

Near Θ (for very small $|z|$), the function h on the right-hand side of eq 4 may be given by[2,6]

$$h = 1 - 2.865\tilde{\tilde{z}} + 8.851\tilde{\tilde{z}}^2 + 5.077\tilde{z}\tilde{\tilde{z}} - ... \tag{7}$$

where the intramolecular and intermolecular scaled excluded-volume parameters $\tilde{z}$ and $\tilde{\tilde{z}}$ are defined by

$$\tilde{z} = (3/4)K(\lambda L)z \tag{8}$$

$$\tilde{\tilde{z}} = [Q(\lambda L)/2.865]z \tag{9}$$

with K and Q being functions only of λL and given by eq 8.46 of ref 2 (or eq 50 of ref 30) and by eq 8.102 of ref 2 (or eq 19 of ref 29) for $\lambda L \gtrsim 1$ (for ordinary flexible polymers), respectively. The conventional excluded-volume parameter z above is now defined by

$$z = (3/2\pi)^{3/2}(\lambda B)(\lambda L)^{1/2} \tag{10}$$

Above Θ ($z > 0$), h is given by eq 8.110 of ref 2 (or eq 18 of ref 29).

Thus, note that h is a function of $\tilde{z}$ and $\tilde{\tilde{z}}$ for $z > 0$ and $z < 0$ and that we may put $h = 1$ approximately for $\lambda L \lesssim 1$. Recall that L is related to M by the equation

$$L = M/M_{\rm L} \tag{11}$$

with $M_{\rm L}$ the shift factor as defined as the molecular weight per unit contour length.

The second term $A_2^{(\rm E)}$ in eq 3 may be written in the form[2,29]

$$A_2^{(\rm E)} = a_1 M^{-1} + a_2 M^{-2} \tag{12}$$

where

$$a_1 = 2N_{\rm A}\beta_1/M_0 \tag{13}$$

$$a_2 = 2N_{\rm A}\Delta\beta_2$$

with M_0 the molecular weight of the bead and with

$$\Delta\beta_2 = \beta_2 - 2\beta_1 \tag{14}$$

The parameters β_1 and β_2 are explicitly defined in eqs 8.117 of ref 2 (or eqs 22 of ref 29). (Note that $\beta_{2,1}$ and $\beta_{2,2}$ in ref 2 are identical with β_1 and β_2, respectively.)

Now, in the oligomer region where the relation $h = 1$ holds, $A_2^{(\rm HW)}$ is independent of M, so that we have, from eqs 3 and 12

$$(A_{2,i} - {\rm A}_{2,j})/(M_i^{-1} - M_j^{-1}) = a_1 + a_2(M_i^{-1} + M_j^{-1}) \tag{15}$$

with $A_{2,i}$ and $A_{2,j}$ the second virial coefficients for the samples with different molecular weights M_i and M_j, respectively. Equation 15 indicates that a_1 and a_2 may be determined from the intercept and slope of the plot of $(A_{2,i} - A_{2,j})/(M_{{\rm w},i}^{-1} - M_{{\rm w},j}^{-1})$ vs $M_{{\rm w},i}^{-1} + M_{{\rm w},j}^{-1}$, respectively. Figure 5 shows such plots with the present data for the low-molecular-weight samples with $M_{\rm w} \leq 2.83 \times 10^3$, for which h may be equated to unity, at the temperatures indicated. We note that the plots at 41.5 °C (Θ) include the data for all the samples given in Table 2, since $A_2^{(\rm HW)} = 0$ at $T = \Theta$ and then eq 15 holds irrespective of the values of $M_{\rm w}$. As in the previous case of a-PS in cyclohexane,[1] the data points at each temperature can be fitted by a straight line, despite the fact that the dependence of A_2 on $M_{\rm w}$ in methyl acetate is different from that in cyclohexane. The results confirm the above statement that the difference in the dependence on $M_{\rm w}$ for low $M_{\rm w}$ between A_2 in the two Θ solvents is due to that between the effects of chain ends. From the straight lines indicated, we have determined a_1 and a_2 at the respective temperatures. It has then been found that a_2 depends on T, although it is independent of T in cyclohexane.[1]

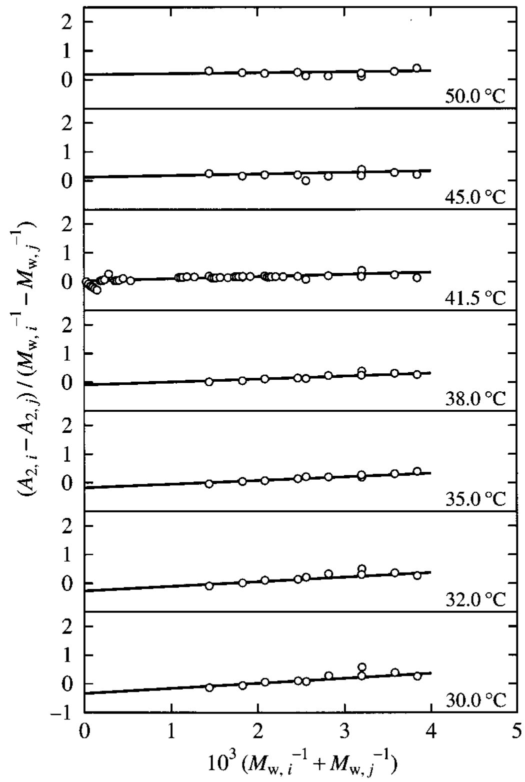

Figure 5. Plots of $(A_{2,i} - A_{2,j})/(M_{{\rm w},i}^{-1} - M_{{\rm w},j}^{-1})$ against $M_{{\rm w},i}^{-1} + M_{{\rm w},j}^{-1}$ for a-PS in methyl acetate at the temperatures indicated (see the text).

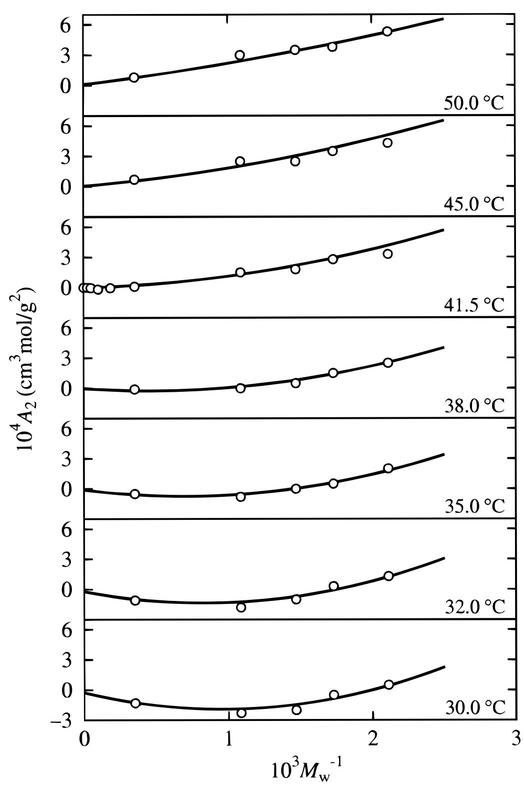

Figure 6. Plots of A_2 against $M_{\rm w}^{-1}$ for a-PS in methyl acetate (see the text).

Figure 6 shows plots of A_2 against $M_{\rm w}^{-1}$ with the data corresponding to those in Figure 5. From the plots, we

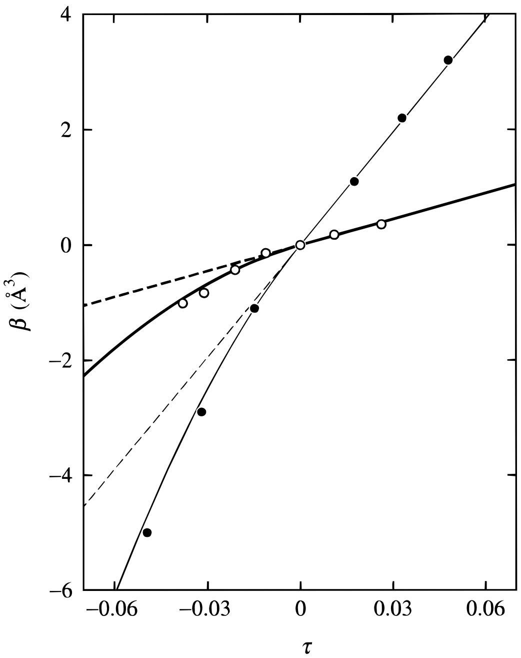

Figure 7. Plots of β against $\tau = 1 - \Theta/T$ for a-PS: (○) present data from A_2 in methyl acetate; (●) previous data from A_2 in cyclohexane.[1] The heavy and light solid curves represent the values calculated from eq 16 and from eq 20 of ref 1, respectively. The heavy and light dashed straight lines are extensions of the heavy and light solid straight lines for $T > \Theta$, respectively (see the text).

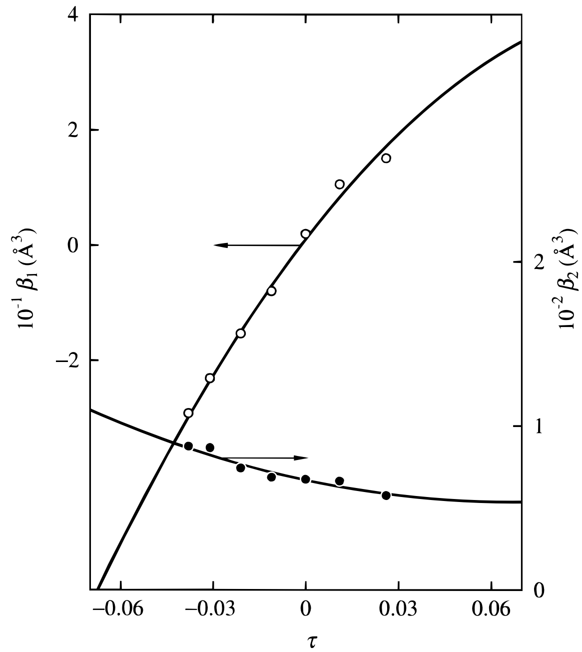

Figure 8. Plots of β_1 and β_2 against τ for a-PS in methyl acetate: (○) β_1; (●) β_2. The solid curves for β_1 and β_2 represent the values calculated from eqs 17 and 18, respectively.

have determined $A_2^{(\mathrm{HW})}$ with $h = 1$ at each temperature so that the curve of A_2 as a function of M_w^{-1}calculated from eqs 3 and 12 with these values of $A_2^{(\mathrm{HW})}$ (with $h = 1$), a_1, and a_2 gives a best fit to the data points. The solid curves in Figure 6 represent the values so calculated. The good agreement between the calculated and observed values indicates again that the dependence of A_2 on M_w for low M_w arises from the effect of chain ends. Note that the intercept of each solid curve is equal to $A_2^{(\mathrm{HW})}$ with $h = 1$, i.e., the prefactor $(N_A c_\infty^{3/2} L^2 B / 2M^2)$, from which we have determined B at the corresponding temperature.

Temperature Dependence of Binary-Cluster Integrals. With the values of B, a_1, and a_2 obtained in the last subsection, we have calculated β, β_1, and β_2 at the respective temperatures from eqs 6 and 13 with eq 14 by taking the repeat unit of the chain as a single bead ($M_0 = 104$). For the calculation of β, we have used the values of the HW model parameters previously[2,7,12] determined from $\langle \Gamma^2 \rangle$ and $\langle S^2 \rangle_0$ for a-PS in cyclohexane at 34.5 °C (Θ), i.e., $\lambda^{-1}\kappa_0 = 3.0$, $\lambda^{-1}\tau_0 = 6.0$, $\lambda^{-1} = 20.6$ Å, and $M_L = 35.8$ Å^{-1}. We note that the value 7.9$_3$ Å^2 of $\lim_{x_w \to \infty} (\langle S^2 \rangle_0 / x_w)$ for a-PS in methyl acetate at 41.5 °C (Θ) evaluated as the mean of the results for the three samples F80a-2, F128a-2, and F288a-2 agrees with the corresponding value 8.13 Å^2 in cyclohexane within experimental error, so that we assume that the values of the model parameters in methyl acetate are the same as those in cyclohexane.

The values of β (in Å^3) obtained at various temperatures above and below Θ are represented by the unfilled circles in Figure 7. It also includes the values previously determined for a-PS in cyclohexane[1] (filled circles) by the same method, for comparison. Although the dependence of β on T is smaller in methyl acetate than in cyclohexane, it is clearly seen that the present data points for $\tau < 0$ deviates downward from a linear extension of the straight line fitted to the data points for $\tau > 0$ (heavy dashed line). The values of β in methyl acetate may be well reproduced by an empirical equation as a function of τ as follows

$$\beta = 15\tau \qquad \text{for } \tau \geq 0$$
$$= 15\tau - 250\tau^2 \qquad \text{for } \tau < 0 \tag{16}$$

The heavy solid curve in Figure 7 represents the values calculated from these equations. In the figure, the light solid curve represents the values calculated from the empirical interpolation formula given by eq 20 of ref 1 in cyclohexane, and the light dashed curve represents a linear extension of the straight-line part for $\tau > 0$.

In Figure 8, the values of β_1 (unfilled circles) and β_2 (filled circles) are plotted against τ. In contrast to the previous case of a-PS in cyclohexane for which both β_1 and β_2 are monotonically increasing functions of τ, in the present case β_1 increases but β_2 decreases with increasing τ. The results explicitly show the difference between the effects of chain ends in the two Θ solvents. The values of β_1 and β_2 in both the Θ solvents are of reasonable order of magnitude as the effective excess binary-cluster integrals associated with the chain end beads compared to those for small molecules.[31] With these results, for later use, we have also constructed empirical equations for β_1 and β_2 (both in Å^3) as functions of τ as follows

$$\beta_1 = 1 + 700\tau - 3000\tau^2 \tag{17}$$

$$\beta_2 = 67 - 400\tau + 3000\tau^2 \tag{18}$$

The solid curves for β_1 and β_2 in Figure 8 represent the values calculated from eqs 17 and 18, respectively.

Dependence of $A_2 M_w^{1/2}$ and $A_2^{(\mathrm{HW})} M_w^{1/2}$ on z. Now we investigate the behavior of the quantities $A_2 M_w^{1/2}$ and $A_2^{(\mathrm{HW})} M_w^{1/2}$ as functions of z. Figure 9 shows plots

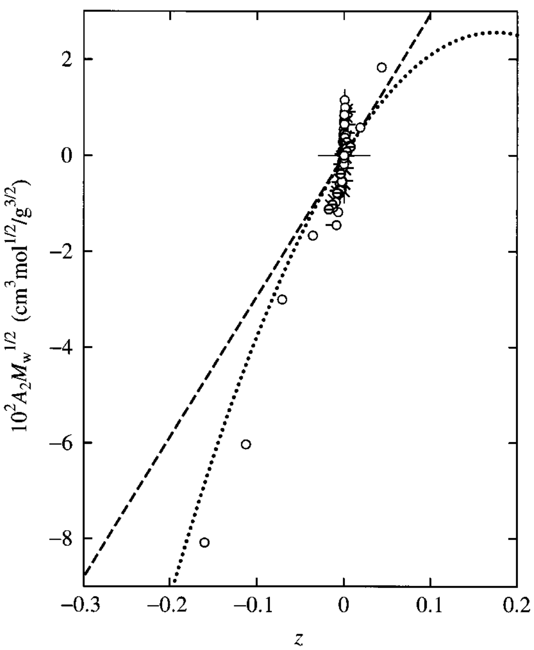

Figure 9. Plots of $A_2M_w^{1/2}$ against z for a-PS in methyl acetate: unfilled circle with pip up, OS4; successive 45° clockwise rotations of pips correspond to OS5, OS6, OS8a, A2500a-2, A5000-3, F1a-2, and F2-2, respectively; (⊖) F4; (○) F850-a. The dashed and dotted curves represent the theoretical values with $A_2^{(E)} = 0$ and $h = 1$ and the first-order TP perturbation theory values, respectively (see the text).

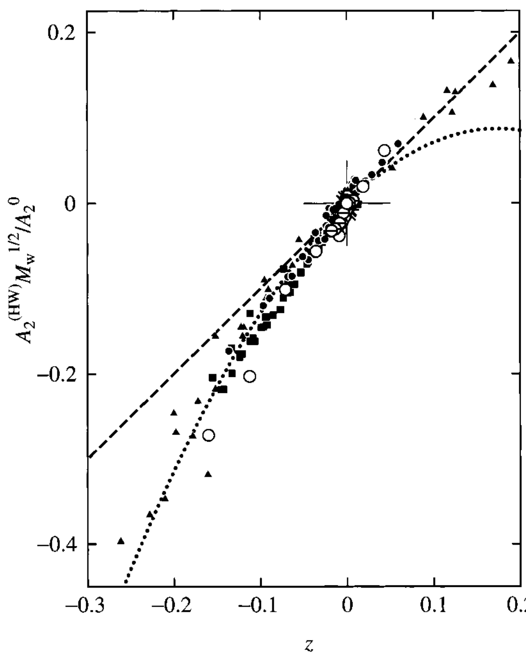

Figure 10. Plots of $A_2^{(HW)}M_w^{1/2}/A_2^0$ against z for a-PS: (⊖, ○) present data in methyl acetate (the symbols and the lines have the same meaning as those in Figure 9); (●) previous data in cyclohexane;[1] (■) Tong et al.'s data for $10^4 \le M_w \le 4.91 \times 10^5$ in cyclohexane;[5] (▲) Miyaki's data for $1.34 \times 10^6 \le M_w \le 3.92 \times 10^7$ in cyclohexane.[33]

of $A_2M_w^{1/2}$ against z with all the data listed in Table 2, where values of z have been calculated from eq 10 with eqs 6 and 16 and with the values of the HW model parameters given above. The dashed straight line represents the theoretical values calculated from

$$A_2^{(HW)}M^{1/2} = A_2^0 z h \tag{19}$$

with $h = 1$ (the TP theory single-contact term), assuming that $A_2^{(E)} = 0$, where A_2^0 is given by

$$A_2^0 = 4(\pi/6)^{3/2} N_A (c_\infty/\lambda M_L)^{3/2} \tag{20}$$

and is calculated to be 0.294 cm^3 mol$^{1/2}$/g$^{3/2}$ with the above values of the HW model parameters.[32] The dotted curve represents the values calculated from eq 19 with the first-order TP perturbation theory of h given by eq 7 with $\tilde{z} = \tilde{\tilde{z}} = z$ (i.e., $h = 1 - 2.865z$). It is seen that the data points cannot form a single-composite curve because of the effect of chain ends (compare with Figure 10 of ref 3).

With the above results for β_1 and β_2, we then evaluate the contribution $A_2^{(E)}$ of the effect of chain ends to A_2 from eq 12 with eqs 13, 14, 17, and 18, and therefore the part $A_2^{(HW)}$ of A_2 without this effect by subtraction of $A_2^{(E)}$ from A_2. Figure 10 shows plots of $A_2^{(HW)}M_w^{1/2}/A_2^0$ against the same z as in Figure 9. Here, the symbols (for the present data) and the lines have the same meaning as those in Figure 9. In the figure, the previous data[1] (filled circles) along with the literature data by Tong et al.[5] for $10^4 \le M_w \le 4.91 \times 10^5$ (filled squares) and by Miyaki[33] for $1.34 \times 10^6 \le M_w \le 3.92 \times 10^7$ (filled triangles) in cyclohexane have been reproduced from Figure 12 of ref 1, for comparison.

It is seen that the peculiar deviation of the $A_2M_w^{1/2}$ vs z plot from the TP theory prediction found in Figure 9 disappears inFigure 10 (compare with Figure 11 of ref 3). This confirms again that the deviation arises from the effect of chain ends. It is more important to see from Figure 10 that all the data points nearly form a single-composite curve. From this result and the previous one for a-PMMA,[3] it may be concluded that the effect of chain stiffness on $A_2^{(HW)}$ and hence A_2 is of little significance below Θ in contrast to the behavior of A_2 above Θ,[2] or in other words, the TP (nearly second-order perturbation) theory is valid for $A_2^{(HW)}$ below Θ irrespective of the differences in polymer species (chain stiffness and local chain corformation) and solvent condition.

Dependence of α_S on $\tilde{z}$. Figure 11 shows plots of $\alpha_S{}^2$ against $\tilde{z}$, where values of $\tilde{z}$ have been calculated from eq 8 with eq 8.46 of ref 2 for K and with the values of z calculated as above. The unfilled circles represent the present values for the sample F850-a in methyl acetate and the unfilled triangles represent the literature values obtained by Chu et al.[20] for $M_w = 2.0 \times 10^6$ and $M_w = 4.6 \times 10^6$ in methyl acetate. There are also plotted the literature data obtained in cyclohexane by Park et al.[34,35] for $4.60 \times 10^6 \le M_w \le 4.09 \times 10^7$ (filled circles) and by Miyaki[33] for $1.34 \times 10^6 \le M_w \le 5.68 \times 10^7$ (filled triangles). The solid curves (1) and (2) represent the first- and second-order perturbation theory values, respectively, calculated from[2,4]

$$\alpha_S{}^2 = 1 + 1.276\tilde{z} - 2.082\tilde{z}^2 + ... \tag{21}$$

It is seen that all the data points again form a single-composite curve within experimental error. This confirms that the QTP theory is valid for α_S below Θ as well as above Θ irrespective of the difference in solvent condition. (Note that $\tilde{z} \simeq z$ for these data.) The composite curve below Θ, which is not shown explicitly, is located between the two curves and is rather close to

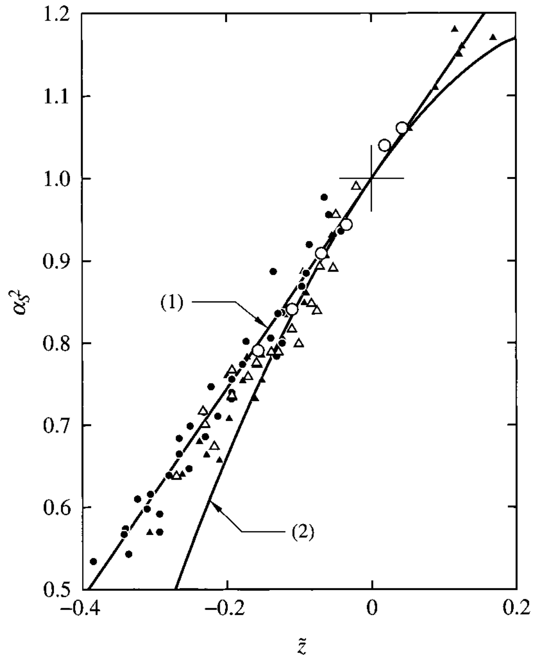

Figure 11. Plots of α_S^2 against $\tilde{z}$ for a-PS: (○) present data for F850-a in methyl acetate; (△) Chu et al.'s data for $M_w = 2.0 \times 10^6$ and $M_w = 4.6 \times 10^6$ in methyl acetate;[20] (●) Park et al.'s data for $4.60 \times 10^6 \leq M_w \leq 4.09 \times 10^7$ in cyclohexane;[34,35] (▲) Miyaki's data for $1.34 \times 10^6 \leq M_w \leq 5.68 \times 10^7$ in cyclohexane.[33] The solid curves (1) and (2) represent the first- and second-order perturbation theory values, respectively.

curve (1) (straight line), i.e., the first-order perturbation theory values, in contrast to $A_2^{(\mathrm{HW})}$.

Conclusion

As in the previous case of a-PS in cyclohexane,[1] A_2 of a-PS in methyl acetate below and above Θ (41.5 °C) has been found to depend appreciably on M_w in the oligomer region. Although the dependence of A_2 on M_w in methyl acetate is different from that in cyclohexane, the former may also be explained quantitatively by the Yamakawa theory[2,29] that takes account of the effect of chain ends, indicating that the difference in the M_w dependence between A_2 in the two Θ solvents arises from that between the effects of chain ends. Then the analysis has allowed us to evaluate the contribution $A_2^{(\mathrm{E})}$ of this effect to A_2 at various temperatures to determine the effective excess binary-cluster integrals β_1 and β_2 associated with the chain end beads in methyl acetate as functions of temperature T. With these values of β_1 and β_2 thus estimated, the binary-cluster integral β between intermediate identical beads has been evaluated as a function of T and found not to be proportional to $\tau = 1 - \Theta/T$ below Θ. With its values, the conventional and scaled excluded-volume parameters z and $\tilde{z}$ have been directly calculated without any assumption.

The part $A_2^{(\mathrm{HW})}$ of A_2 without the effect of chain ends obtained as $A_2^{(\mathrm{HW})} = A_2 - A_2^{(\mathrm{E})}$ below Θ has been found to be consistent with the TP theory prediction, giving a single-composite curve of $A_2^{(\mathrm{HW})}{M_w}^{1/2}$ vs z irrespective of the values of M_w and T and also the difference in solvent condition. This is in contrast to the behavior of $A_2^{(\mathrm{HW})}$above Θ where neither the TP nor QTP theory is valid for it.[2] It has also been found that if α_S is plotted against $\tilde{z}$ (or z for large M_w), the present data points along with those in cyclohexane form a single-composite curve, indicating that the QTP theory is valid for α_S below Θ as well as above Θ irrespective of the difference in solvent condition.

References and Notes

(1) Yamakawa, H.; Abe, F.; Einaga, Y. *Macromolecules* **1994**, *27*, 5704.
(2) Yamakawa, H. *Helical Wormlike Chains in Polymer Solutions*; Springer: Berlin, 1997.
(3) Abe, F.; Einaga, Y.; Yamakawa, H. *Macromolecules* **1995**, *28*, 694.
(4) Yamakawa, H. *Modern Theory of Polymer Solutions*; Harper & Row: New York, 1971.
(5) Tong, Z.; Ohashi, S.; Einaga, Y.; Fujita, H. *Polym. J.* **1983**, *15*, 835.
(6) Yamakawa, H. *Macromolecules* **1993**, 26, 5061.
(7) Konishi, T.; Yoshizaki, T.; Shimada, J.; Yamakawa, H. *Macromolecules* **1989**, *22*, 1921.
(8) Einaga, Y.; Koyama, H.; Konishi, T.; Yamakawa, H. *Macromolecules* **1989**, *22*, 3419.
(9) Abe, F.; Einaga, Y.; Yamakawa, H. *Macromolecules* **1993** *26*, 1891.
(10) Horita, K.; Abe, F.; Einaga, Y.; Yamakawa, H. *Macromolecules* **1993**, *26*, 5067.
(11) Konishi, T.; Yoshizaki, T.; Saito, T.; Einaga, Y.; Yamakawa, H. *Macromolecules* **1990**, *23*, 290.
(12) Abe, F.; Einaga, Y.; Yoshizaki, T.; Yamakawa, H. *Macromolecules* **1993**, 26, 1884.
(13) Koyama, H.; Yoshizaki, T.; Einaga, Y.; Hayashi, H.; Yamakawa, H. *Macromolecules* **1991**, *24*, 932.
(14) Yamada, T.; Yoshizaki, T.; Yamakawa, H. *Macromolecules* **1992**, *25*, 377.
(15) Arai, T.; Abe, F.; Yoshizaki, T.; Einaga, Y.; Yamakawa, H. *Macromolecules* **1995**, *28*, 3609.
(16) Arai, T.; Abe, F.; Yoshizaki, T.; Einaga, Y.; Yamakawa, H. *Macromolecules* **1995**, *28*, 5458.
(17) Yamakawa, H.; Abe, F.; Einaga, Y. *Macromolecules* **1993**, *26*, 1898.
(18) Einaga, Y.; Abe, F.; Yamakawa, H. *Macromolecules* **1993**, *26*, 6243.
(19) Sawatari, N.; Yoshizaki, T.; Yamakawa, H. *Macromolecules* **1998**, *31*, 4218.
(20) Chu, B.; Park, I. H.; Wang, Q.-W.; Wu, C. *Macromolecules* **1987**, *20*, 2833.
(21) Rubingh, D. N.; Yu, H. *Macromolecules* **1976**, *9*, 681.
(22) Einaga, Y.; Abe, F.; Yamakawa, H. *J. Phys. Chem.* **1992**, *96*, 3948.
(23) Abe, F.; Einaga, Y.; Yamakawa, H. *Macromolecules* **1994**, *27*, 3262.
(24) Berry, G. C. *J. Chem. Phys.* **1966**, *44*, 4550.
(25) Bawn, C. E. H.; Freeman, R. F. J.; Kamalidin, A. R. *Trans. Faraday Soc.* **1950**, *46*, 862.
(26) Norisuye, T.; Fujita, H. *ChemTracts—Macromol. Chem.* **1991**, *2*, 293.
(27) Allen, G.; Gee, G.; Mangaraj, D.; Sims, D.; Wilson, G. J. *Polymer* **1960**, *1*, 467.
(28) Höcker, H.; Blake, G. J.; Flory, P. J. *Trans. Faraday Soc.* **1971**, *67*, 2251.
(29) Yamakawa, H. *Macromolecules* **1992**, *25*, 1912.
(30) Shimada, J.; Yamakawa, H. *J. Chem. Phys.* **1986**, *85*, 591.
(31) Yamakawa, H.; Fujii, M. *J. Chem. Phys.* **1973**, 58, 1523.
(32) We note that the value 0.323 for A_2^0 in eq 23 of ref 1, eq 8.161 of ref 2, and eq 25 of ref 6 was calculated with the earlier values[7] of the model parameters. This difference is of minor importance.
(33) Miyaki, Y. Ph.D. Thesis, Osaka University, 1981.
(34) Park, I. H.; Wang, Q.-W.; Chu, B. *Macromolecules* **1987**, *20*, 1965.
(35) Park, I. H.; Fetters, L.; Chu, B. *Macromolecules* **1988**, *21*, 1178.

MA980833Y